Desalination and Water Treatment
www.deswater.com
doi: 10.1080/19443994.2014.937756

56 (2015) 83–96
September

Taylor & Francis
Taylor & Francis Group

Fast artificial neural network (FANN) modeling of Cd(II) ions removal by valonia resin

Ulaş Yurtsever[a,*], Meral Yurtsever[b], İ. Ayhan Şengil[b], Nursel Kıratlı Yılmazçoban[b]

[a]*Department of Computer and Information Engineering, University of Sakarya, Sakarya, Turkey, Tel. +90 264 2955522; Fax: +90 264 2956689; email: ulas@sakarya.edu.tr*
[b]*Department of Environmental Engineering, University of Sakarya, Sakarya, Turkey, Tel. +90 264 2955643; Fax: +90 264 2955601; email: mevci@sakarya.edu.tr (M. Yurtsever), Tel. +90 264 2955631; Fax: +90 264 2955601; email: asengil@sakarya.edu.tr (İ.A. Şengil), Tel. +90 264 2955644; Fax: +90 264 2955601; email: nkiratli@sakarya.edu.tr (N.K. Yılmazçoban)*

Received 19 November 2013; Accepted 4 June 2014

ABSTRACT

In the existing research, firstly, Cd adsorption properties and kinetics were studied on valonia tannin resin (VTR) from aqueous solutions at optimized process parameters such as temperature, pH of solution, initial ion concentration, and contact time. Then, a four-layer fast artificial neural network was constructed and tested to model the equilibrium data of Cd metal ions onto VTR. The properties of the VTR and the experimental conditions were used as inputs to predict the corresponding cadmium uptake at equilibrium conditions. The constructed ANN was also found to be precise in modeling the cadmium adsorption isotherms and kinetics for all inputs during the training process. ANN models were setup with varying numbers of hidden layers and different neuron numbers at each hidden layer as input parameters, mean squared error values were calculated for the train, test, and overtraining caution system status and the proper model according to these values was determined. The obtained simulation results showed that the applied technique of ANN has better adjusted the equilibrium data of the Cd adsorption when compared with the conventional isotherm models.

Keywords: Fast artificial neural networks; Removal; Modeling; Valonia tannin resin; Cd(II) ions

1. Introduction

Removing the heavy metal ions, such as mercury, lead, cadmium, nickel, chromium, copper, zinc, etc., from wastewater is necessary due to their toxic effects on all the living beings. To remove heavy metals effectively from wastewater, scientists developed various physicochemical processes, e.g. chemical precipitation, adsorption, ion exchange, solvent extraction, electrolysis, and membrane techniques (microfiltration, reverse osmosis, and nanofiltration etc.) [1,2]. Currently, the most widely used and effective method for the removal of precious [3,4] and heavy metal ions [5–7] is biosorption. Biosorption has been defined as the property of certain biomolecules (or types of biomass) to bind and concentrate the selected ions or other molecules from aqueous solutions [8].

Many studies have been proposed in the literature about the use of the modified tannin resins, in relation

*Corresponding author.

with heavy metal biosorption from wastewater [9–11]. Tannins have multiple adjacent phenolic hydroxyls and exhibit specific affinity to many precious and heavy metal ions. Tannins are high molecular weight polyphenols that can be found in different parts of plants and trees such as seeds, fruits, roots, and barks.

Artificial neural network (ANN) methods have been applied to many different areas. ANNs have become widely used in various chemical, industrial, computer vision, finance, engineering, health, biological, and environmental research areas, where the available information is experimental [12–16]. ANNs are nets of basis functions; they can provide good empirical models of complex nonlinear processes useful for a wide variety of purposes [17]. ANNs have a number of advantages over the conventional computational systems. The most important advantages are: the capacity of synthesizing complex and transparent mappings, rapidity, robustness, fault tolerance, adaptability, and small memory requirement [18]. Although artificial intelligence applications were not popular in old times, remarkable studies came out in the past decade. The studies about environmental and chemical engineering within the last few years are shown in Table 1.

The performance values, methods used, and results in Table 1 show that the studies on artificial intelligence in recent years has given successful results. In addition, the speed and ability of learning, robustness, predictive abilities, nonlinear characteristics of ANN methods can be combined with the analysis power of statistical methods to prepare models that are more efficient in the solution of problem space. Recently, ANN has been used as a powerful modeling tool in various water and environment studies such as biological decolorization of contaminated water [19], membrane filtration for textile dye wastewater treatment [20], nutrient estimation in a sequencing batch reactor for wastewater treatment [21], the estimation of heavy metal sorption in German soils [13], the prediction of dissolved oxygen and biochemical oxygen demand of the surface water [22], the modeling of the river water quality [23], activated sludge process [24], comparison of ANN approach with 2D and 3D hydrodynamic models for simulating estuary water stage [25], etc. Many researchers used ANN for exhibiting the performance of metal adsorption systems successfully [26–28].

The main aim of the present work is to construct an ANN (ANN) model of Cd^{2+} adsorption onto valonia tannin resin (VTR) and demonstrate its application to isotherm and kinetic data as how it can improve the interpretation of the results.

2. Experimental studies and results

The adsorption experiments were carried out under batch mode at different experimental conditions. The effects of contact time, initial pH, temperature, and initial concentration of cadmium were investigated by varying any of the process parameters and keeping the other parameters constant.

2.1. Batch studies

Batch experiments were performed in a pH range of 2.0–7.0 to determine the effect of initial pH on adsorption. The effect of initial concentration in the solution for six different concentrations of Cd (10, 25, 50, 75, 100, and 150 mg/L) on the adsorption was studied. The effects of various operating temperatures ranging from 293 to 363 K were also investigated in batch studies. When the adsorption was completed, the suspension was filtered and the concentration of Cd^{2+} ion in filtrate was analyzed by atomic absorption spectrophotometer (Shimadzu, AA-6200 type). The adsorption capacity of VTR as milligram per gram of resin (mg/g resin) was calculated by the following equation;

$$q_t = (C_0 - C_t) \times V/W \tag{1}$$

where C_0 is the initial concentration of Cd ions (mg/L), C_t is the metal ion concentrations after adsorption time t (mg/L), V is the volume of metal ion solution (mL) and W is the weight of resin (g). On the basis of batch test results, optimum operating conditions were determined to be an initial pH of 4, an adsorbent dosage of 1.0 g, and a temperature of 363 ± 2 K.

Experimental results showed that a contact time of 30 min was generally sufficient to achieve equilibrium. The effect of experimental parameters such as initial pH, initial Cd(II) concentration, temperature, and contact time were studied and compared with performance of ANN model.

2.2. Isotherm and kinetics

The sorption kinetics of Cd ions onto VTR was studied in batch experiments. The kinetic data were tested using pseudo-first-order, pseudo-second-order, Elovich, and intraparticle diffusion model. The kinetic data were fitted with pseudo-second-order kinetic model. The Langmuir, Freundlich, Temkin, and Dubinin–Radushkevich models were used to describe the equilibrium isotherms. Isotherm studies were carried out with initial concentrations of Cd(II)

Table 1
Comparison of artificial intelligence methods and performance values for environmental and chemical area

The study area and subject	Using artificial intelligence	Adsorption rates	Results and comments	References
Precipitation forecast in specific regions of Greece	Artificial neural networks (ANNs)	–	*The Index of Agreement (IA) ranges between 0.523 and 0.867 and the coefficient of determination (R^2) ranges between 0.141 and 0.603* *Satisfactory precipitation*	[36]
Reservoir operation system	Evolving ANN intelligent system (ENNIS)	–	*The system was capable of successfully, simultaneously, handling various decision variables and provided reasonable and suitable decisions*	[37]
Hydrological systems forecasting	Evolutionary artificial neural network (EANN)	–	*The results indicate the EANN can effectively and efficiently construct a viable forecast module for the 10-day reservoir inflow, and its accuracy is superior to that of the AR and ARMAX models*	[38]
Groundwater level forecasting in a river island of Eastern India	Gradient descent with momentum and adaptive learning rate backpropagation (GDX) algorithm, Levenberg–Marquardt (LM) algorithm, Bayesian regularization (BR) algorithm	–	*Developed ANN models are capable of predicting weekly groundwater levels over the study area reasonably well even for higher lead times*	[39]
Modeling Ligvanchai watershed rainfall–runoff process at Tabriz, Iran.	A multivariate ANN-wavelet approach for rainfall hybrid wavelet–artificial neural network (WANN) model	–	*ANN nonlinear calibration R^2 0.80, verification R^2 0.74* *WANN hybrid calibration R^2 0.95, verification R^2 0.92* *Modeling rainfall–runoff process by conjunction of the proposed model and fuzzy logic can be a good idea for the future research*	[40]
Predict the effluent concentrations of BOD and SS for a wastewater treatment plant	Artificial neural network (ANN)	–	*The neural network models provided good estimates for the BOD and SS data sets*	[41]
Engineered floodplain filtration system operation	Artificial neural network (ANN) based on multilayer perceptrons with back propagation algorithm	–	*Determination coefficient (R^2) value (≥0.99) achieved during prediction of the testing set* *The model was adequately trained with the laboratory-scale EFF column data and tested with a separate data-set*	[42]
The sorption kinetics of pentachlorophenol (PCP) to sediments	Radial basis function neural network (RBFN) and adaptive neuro-fuzzy inference system (ANFIS)	–	*Both RBFN and ANFIS can get high correlation coefficient (r) and low standard errors as compared with the experimental data for all the eight different sediments*	[43]
Predicting of metallurgical performance (grade and recovery) in pilot flotation column	Artificial neural networks (ANN) and multivariate non-linear regression (MNLR) models	–	*R values for testing the set of Cu grade and recovery as well as Mo grade and recovery were 0.92, 0.92, 0.92, and 0.89, respectively* *Results were quite satisfactory*	[44]

(*Continued*)

Table 1 (*Continued*)

The study area and subject	Using artificial intelligence	Adsorption rates	Results and comments	References
Prediction of *adsorption of* Cd^{2+} by hematite (pH 9, 20°C, 1 h)	Adapted neural fuzzy model and a back propagation artificial neural network	62.27 μmol/L (ANN pred. 53.057 μmol/L ANFIS pred. 62.373)	*The adaptive neuro-fuzzy inference system proved to be more efficient in predicting Cd adsorption than a single-layered feed-forward artificial neural network*	[45]
Cu^{2+} *Adsorption* light expended clay aggregate (LECA) (pH 5, 50°C, 3 h, initial concentration 150 mg/L, ads.dosage 150 mg)	Response surface methodology (RSM) and artificial neural network (ANN)	34.153 mg/g (ANN pred. 37.762 mg/g, from Lang.113.636 mg/g)	A comparison between the model results and experimental data gave a high correlation coefficient ($R^2_{ANN} = 0.962$, $R^2_{RSM} = 0.941$) *Two models were able to predict* Cu^{2+} *removal by LECA*	[46]
Biosorption of immobilized Bacillus subtilis beads (IBSB) for Cd^{2+} *ions* (pH 5.91, 45°C, 3 h, initial concentration 496.23 mg/L)	Artificial neural network (ANN)	251.91 mg/g	The applied model successfully predicted cadmium biosorption capacity with determination coefficient of 0.997 *ANN model can be used for the simulation of batch biosorption process for IBSB*	[47]
Adsorption of sodium dodecyl benzene sulfonate (SDBS) onto polyaniline (PANI) (PANI doped with $CuCl_2$ pH 2, PANI doped with $CuCl_2$ pH 3), (initial concentration 100 mg/L, ads. dosage 0.5 g, 23°C)	Multi linear regression and artificial neural networks	(PANI doped with $CuCl_2$ 32.3 mg/g, PANI doped with $CuCl_2$ 29.5 mg/g)	*Results of ANN applications demonstrated that a backpropagation feed-forward network type with two hidden layers provided successful modeling efficiencies for both of the PANI species*	[48]
Cr(VI) adsorption by zeolite prepared from raw fly ash (ZFA) (pH 2, 4 h, 0.3 g/50 mL, 20°C)	Artificial neural network (ANN)	37.3 mg/g	As a result of using the ANN model, the values of the determination coefficient (R^2) and the mean square error (MSE) were found to be 0.98 and 0.00027364, respectively *ANN model can estimate the behavior of the Cr(VI) removal process under different conditions*	[49]
Arsenic(III) biosorption by living cells of Bacillus cereus biomass (pH 7.5, 30°C, 1.5 h)	Artificial neural network (ANN)	32.42 mg/g	Comparison between the model results and experimental data gives a high degree of correlation ($R^2 = 0.986$) *The model is able to predict the sorption efficiency with reasonable accuracy*	[50]
Cd^{2+} *ions adsorption* on valonia tannin resin (VTR) (pH 4, 20–25°C, 3 h)	Fast artificial neural network	(ANN pred. 62.56 mg/g) (from Langmuir 63.291 mg/g)	*The experimental results obtained from laboratory studies and the mathematical results calculated from isotherm and kinetic equations completely match with the ANN results found.*	Current studies

Table 2
Langmuir, Freundlich, Tempkin, and Dubinin–Radushkevich isotherm constants for the adsorption of Cadmium ion onto VTR (at 296 ± 2 K, pH = 4)

		Langmuir isotherm				Freundlich isotherm			Tempkin isotherm			Dubinin–Radushkevich isotherm		
		a_L (L/mg)	K_L (L/g)	Q_0 (mg/g)	R^2	K_F (L/g)	n	R^2	B	A (L/g)	R^2	q_m (mmol/g)	β (mmol^2/j^2)	R^2
Valonia	Cd^{+2}	0.267	16.920	63.291	0.995	18.793	2.539	0.925	9.029	10.894	0.997	410.141	−3E−06	0.839

ranging from 10 to 150 mg/L. The adsorption process was conducted at 296 ± 2 K with 350 rpm constant stirring for 180 min. The maximum adsorption capacity of Cd^{2+} was obtained 63.291 mg g^{-1} at 296 ± 2 K. Table 2 summarizes Cd adsorption isotherms measured at optimum pH (using 38–53 μm particle size, 296 ± 2 K). From Table 2, it was observed that the best fitting linear expressions were the Langmuir and Tempkin isotherms.

In order to investigate the kinetics of Cd adsorption, the kinetic data shown in Table 3 were analyzed by the intraparticle diffusion, pseudo-first-order, pseudo-second-order, and Elovich kinetic model equations. The second-order equation appeared to be the better-fitting model than other equations because it has the higher R^2 (0.998). The equilibrium adsorption capacity calculated by pseudo-second-order model and that determined by actual measurement are very closed to each other (Fig. 7).

3. Construction studies of ANN

Generally, the analysis of the performance of various processes is based on deterministic mathematical models and the successful development of a theoretical model relies on the availability of good process information [29].

In this study, 456 experiments were conducted to study the Cd adsorption on the tannin resin, and the obtained data were used for ANN prediction model. In addition, an attempt has been made to apply an ANN to predict the biosorption of Cd ions with modified tannin resin under different operating conditions, such as initial concentration of Cd(II) ions, initial pH, operating temperature, and contact time.

ANN technique was used in comparing the results with those from multiple regression analysis and the experimental studies. Six different input parameters were used in order to determine the adsorption percentage and 456 different experiments were made using these input parameters; adsorption amount was determined for each experiment. All of the parameters to be used for ANN approach were composed of numeric values. The operating range and data statistic of the input variables are shown Table 4.

First, correlation analysis was applied to the data for which data statistics information has been given in Table 4 and the relationship between these parameters has been given in Table 5. It has been observed in this correlation analysis that input parameters, such as initial concentration of Cd(II) ions, initial pH, operating temperature, and contact time have no correlation with each other and with the output parameters. High correlation is observed between initial concentration

Table 3
Kinetic parameters for the sorption of Cd^{2+} on VTR

		Intraparticle diffusion model		Pseudo-first-order kinetic model		Pseudo-second-order kinetic model		Elovich equation		
Pb^{+2} C_0 (mg/L)	q_e (mg/g)	k_{int} (mg/g.min$^{1/2}$)	R^2	k_1 (1 min^{-1})	R^2	k_2 (g/mg.min)	R^2	α (mg/g.min)	β (g min^{-1})	R^2
10	9.692	0.3014	0.891	0.0308	0.957	0.0253	0.9980	9.149E+02	1.2583	0.962
25	23.862	0.5713	0.556	0.0297	0.574	0.0454	0.9999	1.684E+04	0.5676	0.821
50	41.934	0.5043	0.909	0.0134	0.923	0.0178	0.9997	2.370E+11	0.7504	0.985
75	49.803	0.8772	0.808	0.0164	0.850	0.0120	0.9994	1.221E+07	0.4143	0.949
100	55.160	1.1457	0.955	0.0302	0.914	0.0049	0.9980	6.450E+06	0.3709	0.821
150	62.179	0.2182	0.883	0.0151	0.907	0.0387	1.0000	7.204E+43	1.7224	0.971

Table 4
Data statistics of input variables

Variable	Mean	Std. error	Median	Std. deviation	Sample variance	Kurtosis	Skewness	Range	Min.	Max.	Count
Initial pH	4.11	0.04	4	0.81	0.66	5.62	1.39	5	2	7	455
Temperature	25.63	0.76	20	16.26	264.31	7.93	3.00	70	20	90	455
Agitation rate	358.09	4.56	350	97.37	9481.58	13.29	2.83	670	130	800	455
Particle size	45.81	1.11	38	23.75	564.11	11.20	3.42	112	38	150	455
Cd initial concentration	32.42	1.67	10	35.57	1265.07	3.10	1.85	140	10	150	455
Contact time	66.88	2.59	50	55.26	3054.18	−0.85	0.65	179	1	180	455
Adsorption rate	22.07	0.85	9.62	18.12	328.44	−1.10	0.71	60.19	1.99	62.18	455

Table 5
Correlation analysis

	Initial pH	Temperature	Agitation rate	Particle size	Cd initial concentration	Contact time	Adsorption rate
Initial pH	1.0000						
Temperature	−0.0451	1.0000					
Agitation rate	−0.0108	−0.0288	1.0000				
Particle size	−0.0428	−0.1141	−0.0274	1.0000			
Cd initial concentration	−0.0821	0.1715	−0.0525	−0.2077	1.0000		
Contact time	0.0081	0.0215	0.0052	0.0273	−0.0671	1.0000	
Adsorption rate	−0.0394	0.4323	−0.0571	−0.2415	0.9077	−0.0091	1.0000

and the amount of adsorption. Initial concentration is absorbed substantially; therefore, correlation is expected to be high.

The multiple regressions analysis was made for the whole experiment data-set by using different combinations between input parameters. The input parameters used in the ANN model were determined with this analysis. The real values and analysis results values were analyzed statistically and these values were counted in order of determination of coefficient (R^2), Std. error, Sig. F, mean squared error (MSE), root mean square error (RMSE), mean absolute error (MAE), median absolute error (MEDAE), and average absolute relative error (AARE). According to these values, input combination, whose R^2 value was approximately 1 and tolerance was low, was defined and showed in Table 6. This input combination is used like the ANN model's input parameter.

where p1 is the initial pH, p2 is the temperature, p3 is the agitation rate, p4 the is particle size, p5 is the Cd initial concentration, and p6 is the contact time. Normalization is a very critical issue in ANN.

Table 6
The results of regression analysis to determine the input parameters of ANN

	R^2	Std. error	Sig. F	MSE	RMSE	MAE	MEDAE	AARE
p1	0.001	18.13	0.40	327.21	18.09	16.56	13.17	162.53
p1 + p2	0.19	16.37	0.00	266.35	16.32	13.78	9.99	133.64
p1 + p2 + p3	0.19	16.37	0.00	265.69	16.30	13.74	10.25	133.63
p1 + p2 + p3 + p4	0.23	16.00	0.00	253.08	15.91	13.28	11.22	135.54
p1 + p2 + p3 + p4 + p5	0.91	5.60	0.00	30.92	5.56	4.11	2.59	38.95
p1 + p2 + p3 + p4 + p5 + p6	0.91	5.55	0.00	30.32	5.51	4.05	2.53	38.73
p1 + p2 + p3 + p4 + p6	0.23	16.01	0.00	253.03	15.91	13.27	11.16	135.45
p1 + p2 + p3 + p5	0.90	5.62	0.00	31.19	5.58	4.11	2.59	37.88
p1 + p2 + p3 + p5 + p6	0.91	5.57	0.00	30.60	5.53	4.06	2.37	37.76
p1 + p2 + p3 + p6	0.19	16.39	0.00	265.58	16.30	13.73	10.38	133.54
p1 + p2 + p4	0.23	16.01	0.00	253.93	15.94	13.33	11.14	135.54
p1 + p2 + p4 + p5 + p6	0.91	5.54	0.00	30.32	5.51	4.05	2.52	38.69
p1 + p2 + p5	0.90	5.61	0.00	31.19	5.59	4.11	2.58	37.86
p1 + p2 + p6	0.19	16.39	0.00	266.24	16.32	13.78	10.16	133.55
p1 + p3	0.004	18.12	0.33	326.13	18.06	16.49	13.83	162.40
p1 + p3 + p4	0.06	17.58	0.00	306.44	17.51	15.76	14.74	163.05
p1 + p3 + p4 + p5	0.83	7.55	0.00	56.34	7.51	5.92	3.98	53.77
p1 + p3 + p4 + p5 + p6	0.83	7.49	0.00	55.43	7.45	5.85	4.02	53.40
p1 + p3 + p4 + p6	0.06	17.60	0.00	306.44	17.51	15.76	14.78	163.04
p1 + p3 + p5	0.83	7.60	0.00	57.24	7.57	5.96	3.76	52.26
p1 + p3 + p6	0.00	18.14	0.53	326.11	18.06	16.49	13.87	162.37
p1 + p4	0.06	17.60	0.00	307.80	17.54	15.84	14.16	163.17
p1 + p4 + p5	0.83	7.54	0.00	56.38	7.51	5.93	3.97	53.71
p1 + p4 + p5 + p6	0.83	7.49	0.00	55.47	7.45	5.86	3.99	53.34
p1 + p4 + p6	0.06	17.62	0.00	307.80	17.54	15.84	14.18	163.16
p1 + p5	0.83	7.59	0.00	57.27	7.57	5.97	3.74	52.23
p1 + p5 + p6	0.83	7.54	0.00	56.39	7.51	5.90	3.84	51.92
p1 + p6	0.00	18.15	0.69	327.19	18.09	16.56	13.32	162.50
p2	0.19	16.36	0.00	266.48	16.32	13.81	10.03	131.96
p2 + p3	0.19	16.36	0.00	265.82	16.30	13.77	10.32	131.90
p2 + p3 + p4	0.23	15.99	0.00	253.37	15.92	13.33	11.35	133.00
p2 + p3 + p4 + p5	0.90	5.64	0.00	31.50	5.61	4.08	1.64	42.90
p2 + p3 + p4 + p6	0.23	16.00	0.00	253.32	15.92	13.32	11.43	132.92
p2 + p3 + p5	0.90	5.67	0.00	31.83	5.64	4.07	1.62	41.96
p2 + p3 + p6	0.19	16.37	0.00	31.83	5.64	4.07	1.62	41.96
p2 + p4	0.22	16.00	0.00	254.21	15.94	13.38	11.16	133.05
p2 + p4 + p5	0.90	5.64	0.00	31.51	5.61	4.08	1.63	42.88
p2 + p4 + p6	0.22	16.01	0.00	254.16	15.94	13.38	11.21	132.97
p2 + p5	0.90	5.66	0.00	31.83	5.64	4.07	1.58	41.94
p2 + p5 + p6	0.90	5.61	0.00	31.24	5.59	4.02	2.03	41.75
p2 + p6	0.19	16.37	0.00	266.37	16.32	13.81	10.20	131.89
p3	0.00	18.11	0.22	326.65	18.07	16.57	13.75	159.15
p3 + p4	0.06	17.59	0.00	307.28	17.53	15.86	14.77	158.91
p3 + p4 + p5	0.83	7.56	0.00	56.67	7.53	5.89	3.15	56.71
p3 + p4 + p5 + p6	0.83	7.51	0.00	55.76	7.47	5.82	3.66	56.32
p3 + p4 + p6	0.06	17.61	0.00	307.28	17.53	15.86	14.77	158.90
p3 + p5	0.82	7.62	0.00	57.65	7.59	5.93	3.02	55.46
p3 + p5 + p6	0.83	7.57	0.00	56.76	7.53	5.86	3.52	55.14
p3 + p6	0.00	18.13	0.47	326.63	18.07	16.56	13.81	159.12
p4	0.06	17.61	0.00	308.61	17.57	15.93	14.18	159.09
p4 + p5	0.83	7.56	0.00	56.72	7.53	5.90	3.10	56.67
p4 + p5 + p6	0.83	7.50	0.00	55.81	7.47	5.82	3.72	56.28

(*Continued*)

Table 6 (*Continued*)

	R^2	Std. error	Sig. F	MSE	RMSE	MAE	MEDAE	AARE
p4 + p6	0.06	17.63	0.00	308.61	17.57	15.93	14.21	159.08
p5	0.82	7.61	0.00	57.68	7.59	5.93	3.02	55.43
p5 + p6	0.83	7.56	0.00	56.79	7.54	5.87	3.58	55.12
p6	0.00	18.14	0.85	327.70	18.10	16.63	13.28	159.30

Note: Selected italic values (p1+p2+p3+p4+p5+p6) represent the best combination of input values for ANN.

Normalization has a major role in the training and testing of neural networks [30]. Therefore, experimental data-sets are scaled between 0.1 and 0.9 using the normalization equation below in order to reduce dimensional effects of the input parameters in different ranges of values with keeping the relationship between dependent and independent variables.

$$X_n = 0.1 + 0.8 \times (X - X_{min})/(X_{max} - X_{min}) \quad (2)$$

where X_n is the normalized value of the corresponding X, X_{min} is the minimum values of X, and X_{max} is the maximum values of X.

The data, which are obtained from experimental works about absorption in the lab, are normalized and then divided into two sections. One section has 20% and this section is test data, and the second section has 80%, which will be training data. These input parameters are used in different combinations such as 1 hidden layer, 2 hidden layers, 3 hidden layers and every hidden layer has neurons, whose numbers are different from each other. The ANN models are established with these various combinations. With the result of educated ANN models, training MSE values, and testing MSE values are obtained into three categories. Overtraining caution system (OCS), which is into

Table 7
The number of layers and neurons for ANN model

	Minimum training MSE		Minimum testing MSE		Minimum OCS MSE	
Layer and neuron number	Training MSE	Testing MSE	Training MSE	Testing MSE	Training MSE	Testing MSE
5	2.03E−05	3.24E−05	2.03E−05	3.24E−05	2.03E−05	3.24E−05
10	9.99E−06	1.69E−05	1.02E−05	1.55E−05	1.02E−05	1.55E−05
15	1.11E−05	1.92E−05	1.15E−05	1.75E−05	1.14E−05	1.75E−05
20	1.10E−05	2.01E−05	1.15E−05	1.62E−05	1.15E−05	1.62E−05
25	2.16E−05	3.55E−05	2.22E−05	3.47E−05	2.22E−05	3.47E−05
5–5	3.59E−05	5.55E−05	3.72E−05	5.45E−05	3.62E−05	5.50E−05
10–5	8.09E−06	1.44E−05	8.45E−06	1.41E−05	8.11E−06	1.43E−05
15–5	8.13E−06	1.46E−05	8.61E−06	1.33E−05	8.61E−06	1.33E−05
20–5	5.68E−06	9.79E−06	6.51E−06	8.00E−06	6.51E−06	8.00E−06
25–5	*3.28E−06*	*8.18E−06*	*4.32E−06*	*6.27E−06*	*3.36E−06*	*6.51E−06*
10–10	1.60E−05	2.61E−05	1.93E−05	2.56E−05	1.61E−05	2.57E−05
15–15	7.88E−06	1.48E−05	7.88E−06	1.48E−05	7.88E−06	1.48E−05
20–20	8.64E−06	1.31E−05	8.64E−06	1.31E−05	8.64E−06	1.31E−05
25–25	1.54E−05	3.14E−05	1.58E−05	3.02E−05	1.58E−05	3.02E−05
5–5–5	6.81E−06	1.24E−05	7.12E−06	1.20E−05	7.12E−06	1.20E−05
10–5–5	5.22E−06	1.25E−05	5.22E−06	1.25E−05	5.22E−06	1.25E−05
10–10–5	5.16E−06	8.75E−06	5.30E−06	8.46E−06	5.30E−06	8.46E−06
10–10–10	4.85E−06	1.17E−05	4.97E−06	8.47E−06	4.97E−06	8.47E−06
15–10–10	5.19E−06	7.17E−06	5.72E−06	7.08E−06	5.19E−06	7.17E−06
15–15–10	4.40E−06	1.48E−05	4.70E−06	9.07E−06	4.70E−06	9.07E−06
15–15–15	4.68E−06	9.92E−06	5.27E−06	8.77E−06	4.73E−06	9.01E−06
20–15–15	6.63E−06	1.57E−05	6.63E−06	1.57E−05	6.63E−06	1.57E−05
20–20–15	4.42E−06	1.29E−05	4.81E−06	1.16E−05	4.81E−06	1.16E−05
20–20–20	5.16E−06	9.15E−06	5.51E−06	7.62E−06	5.51E−06	7.62E−06
25–20–20	7.67E−06	1.38E−05	8.25E−06	9.16E−06	8.25E−06	9.16E−06
25–25–20	5.54E−06	1.26E−05	7.94E−06	7.86E−06	7.94E−06	7.86E−06

Note: Selected italic values(25-5) represent the best combination of the number of neurons and layers for the ANN model.

Table 8
Details of the trained neural network used to predict the Cd ion adsorption

Type	Value/comment
Layer 1 (input)	6 neurons
Layer 2 (hidden)	25 neurons
Layer 3 (hidden)	5 neurons
Layer 4 (output)	1 neuron
Number of data used for training	366
Number of data used for testing	90
Function in training	FANN_TRAIN_RPROP
Function in hidden layer	FANN_ELLIOT
Function in output layer	FANN_SIGMOID_SYMMETRIC

three different categories is a system that prevents over memorization of ANN. Here, OCS-MSE values are optimum error values and here ANN does not over memorize. In light of these values, convenient numbers of layers and neurons are defined to ANN model and analysis results, which are made before the definition of ANN model, are shown in Table 7.

The model with the lowest error values is determined by testing the ANN models which have different layers and different neuron counts. The details of the ANN model determined are shown in Table 8.

As shown in Fig. 1, the model consists 4 layers: an input layer, two hidden layers, and an output layer. FANN_ELLIOT and FANN_SIGMOID_SYMMETRIC functions are used in the hidden layers and the output layer, respectively.

In the determined ANN model, fast artificial neural network (FANN)'s FANN_TRAIN_RPROP function [31] is used as a training function, FANN_ELLIOT function is used in the hidden layer and FANN_ SIGMOID_SYMETRIC function is used in the output layer. There are 456 experimental data-sets that are obtained for adsorption studies. Three hundred and sixty-six of these are used for training and 90 are used for testing. This function is a highly developed version of the batch training method and does not use the speed of learning due to its characteristics. This method was firstly developed by Riedmiller and Braun in 1993. IRPROP, which is used in the FANN, is a variant of Resilient Backpropagation (RPROP), which is developed by Igel and Hüsken [32–35].

For training and testing of the proposed ANN model, FANNTool 1.4 which is software of the FANN was used. The proposed FANNTool software is free open-source software. This software was preferred because it produces fast results; it is also simple, and easy to use.

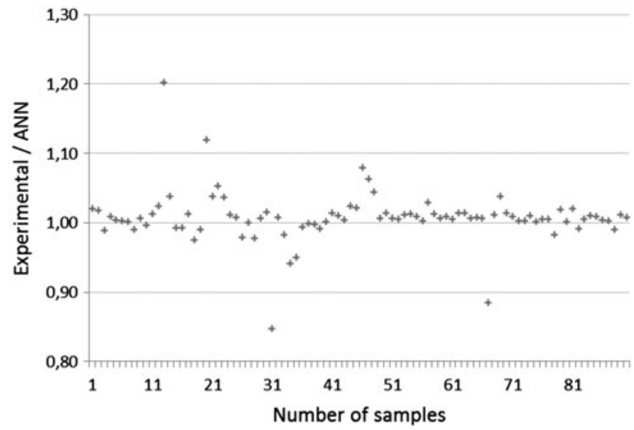

Fig. 2. Ratio of experimental results to the ANN results.

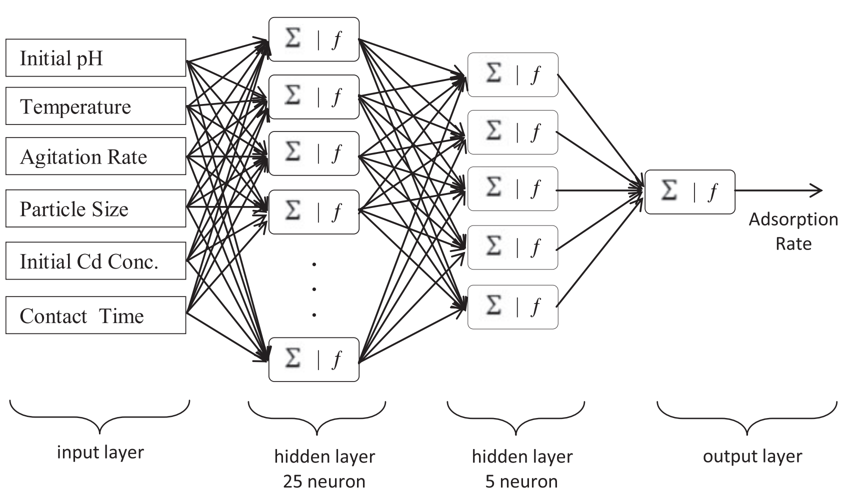

Fig. 1. Topology of the ANN.

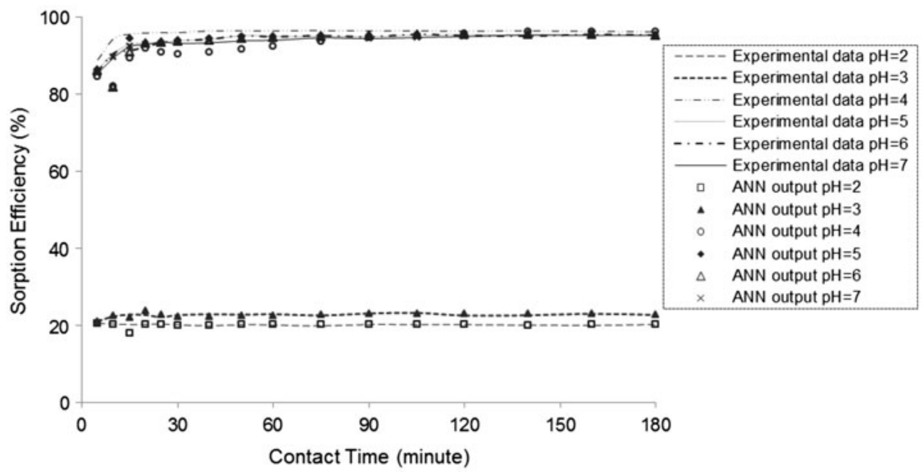

Fig. 3. Agreement between ANN outputs and experimental data as a function of initial pH (VTR dosage = 1.0 g, initial Cd ions concentration = 10 mg/L, and temperature = 293 K).

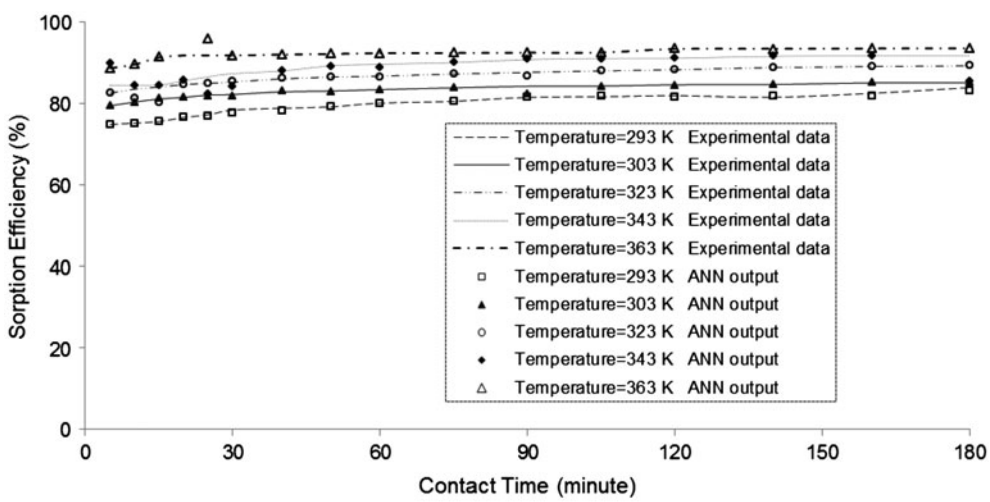

Fig. 4. Agreement between ANN outputs and experimental data as a function of temperature (VTR dosage = 1.0 g, initial Cd ions concentration = 10 mg/L, and pH = 4).

4. ANN modeling and results

A model based on an ANN was constructed to model Cd^{2+} concentration removed from aqueous solution as a function of empirical parameters, and we investigated the possibility of training ANN models correlating the Cd adsorption input variables (independent) with their output variable (dependent variable). The model with the lowest error was determined by testing ANN models with different numbers of layers and neurons. Accordingly, it was found that the two hidden-layered ANN models with 25 neurons in layer 1 and 5 neurons in layer 2 have the lowest MSE values. Therefore, the model given in Table 8 was used for the ANN.

The value of R^2, which was calculated using the ANN test data plotted in the graph corresponding to the data used for testing, was 0.999. Additionally, the graph showing the ratio of the experimental data and the ANN test data are given in Fig. 2. In conclusion, it is observed that the experimental results and the ANN test data obtained from the ANN model are similar.

The results obtained from the experimental studies and the ANN test results were compared for the different PH values of 2, 3, 4, 5, 6, and 7; the temperatures of 293, 303, 323, 343, and 363 K and the initial concentrations of 15, 25, 50, 75, 100 mg/L, NS 150 mg/L and ARE given in Figs. 3–5, respectively. What is more,

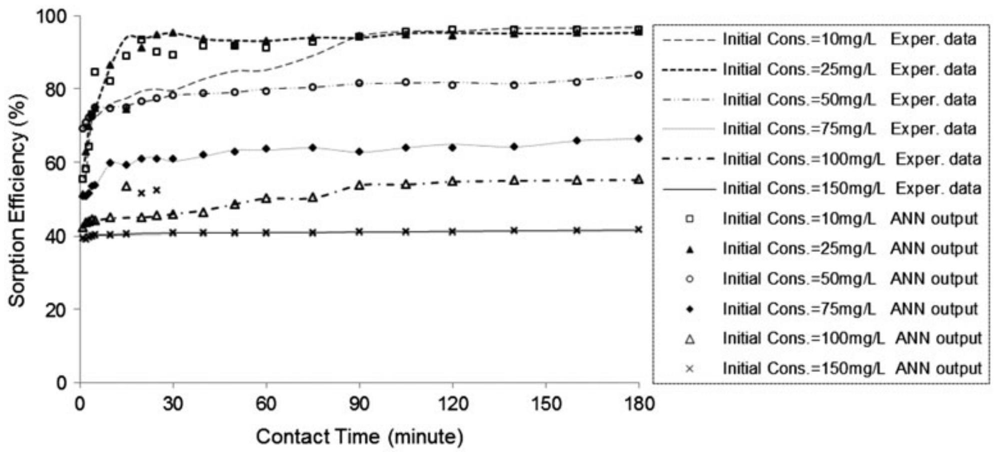

Fig. 5. Agreement between ANN outputs and experimental data as a function of initial Cd concentration (VTR dosage = 1.0 g and pH = 4, and temperature = 293 K).

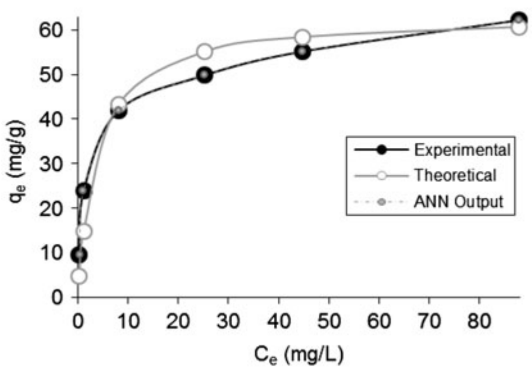

Fig. 6. Agreement between ANN outputs, theoretical, and experimental data for Langmuir isotherm data.

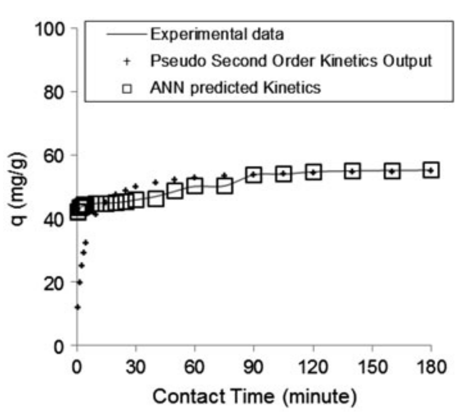

Fig. 7. Agreement between ANN outputs, theoretical, and experimental data for second-order kinetic results.

these experimental results were mathematically calculated according to the Langmuir isotherm and pseudo-second-order kinetics. All the obtained results are shown in Figs. 6 and 7, comparatively. According to these results, ANN results were found to be consistent with the experimental and mathematical results.

In conclusion, the prediction equation of the ANN model created using normalized values of data obtained from our laboratorial experiments on adsorption is calculated as follows.

$$Y = -3.64 + 0.94\text{p1} + 0.31\text{p2} - 0.0008\text{p3} - 0.023\text{p4} + 0.44\text{p5} + 0.01\text{p6} \quad (3)$$

where p1 is the initial pH, p2 is the temperature, p3 is the agitation rate, p4 is the particle size, p5 is the Cd initial concentration, and p6 is the contact time.

The consistency of experimental data and ANN test data are shown in Fig. 8. These results show that the ANN adsorption data and experimental data are consistent.

5. Conclusions

On the basis of batch experimental results, optimal operating conditions were determined to be an initial pH of 4, an adsorbent dosage of 1.0 g, an initial Cd(II) concentration of 10 mg/L, and a temperature of 293 ± 2 K.

In this study, a four-layer ANN model consisting of an input layer, two hidden layers, and an output layer was used, and the appropriate input parameters for this model were determined by regression analysis.

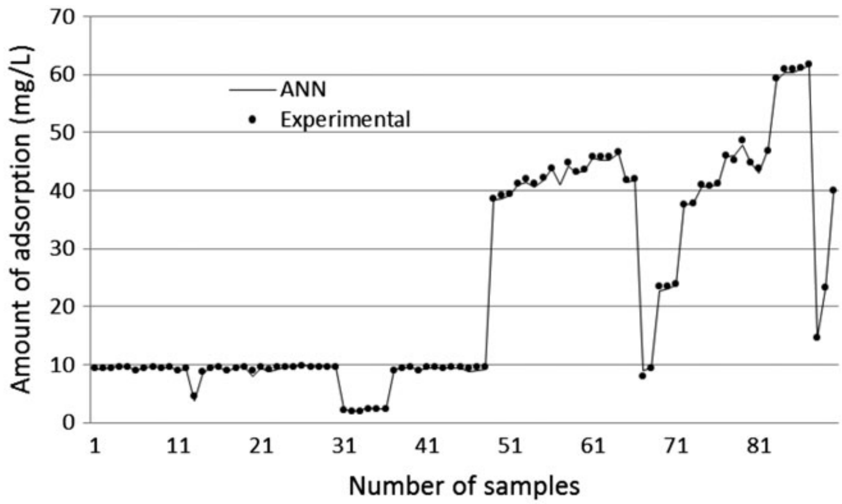

Fig. 8. Consistency between experimental data and ANN test data.

This ANN model demonstrated a precise and effective prediction with a correlation coefficient and MSE of about 0.9997 and 6.51E-6, respectively for the removal of Cd(II) ions. The RPROP was selected because of a fast and accurate train function. The optimum count of hidden layers for RPROP training function was decided to be 2, and the counts of neurons in these two layers were decided to be 25 and 2, respectively. As a result, it has been observed that the experimental results obtained from laboratory studies and the mathematical results calculated from isotherm and kinetic equations completely match with the ANN results found. In addition, consistency rate of the ANN and the experimental results are observed to be close to 1.

Acknowledgments

This work has been supported by The Scientific and Technological Research Council of Turkey. The authors would like to present their deepest thanks TUBITAK for its financial support.

References

[1] S. Ricordel, S. Taha, I. Cisse, G. Dorange, Heavy metals removal by adsorption onto peanut husks carbon: Characterization, kinetic study and modeling, Sep. Purif. Technol. 24 (2001) 389–401.
[2] R. Petrus, J.K. Warchoł, Heavy metal removal by clinoptilolite. An equilibrium study in multi-component systems, Water Res. 39 (2005) 819–830.
[3] N. Das, Recovery of precious metals through biosorption—A review, Hydrometallurgy 103 (2010) 180–189.
[4] C. Mack, B. Wilhelmi, J.R. Duncan, J.E. Burgess, Biosorption of precious metals, Biotechnol. Adv. 25 (2007) 264–271.
[5] E. Fourest, J.C. Roux, Heavy metal biosorption by fungal mycelial by-products: Mechanisms and influence of pH, Appl. Microbiol. Biotechnol. 37 (1992) 399–403.
[6] T.A. Davis, B. Volesky, A. Mucci, A review of the biochemistry of heavy metal biosorption by brown algae, Water Res. 37 (2003) 4311–4330.
[7] L. Velásquez, J. Dussan, Biosorption and bioaccumulation of heavy metals on dead and living biomass of *Bacillus sphaericus*, J. Hazard. Mater. 167 (2009) 713–716.
[8] B. Volesky, Biosorption and me, Water Res. 41 (2007) 4017–4029.
[9] M. Yurtsever, İ.A. Şengil, Biosorption of Pb(II) ions by modified quebracho tannin resin, J. Hazard. Mater. 163 (2009) 58–64.
[10] İ.A. Şengil, M. Özacar, Biosorption of Cu(II) from aqueous solutions by mimosa tannin gel, J. Hazard. Mater. 157 (2008) 277–285.
[11] X. Huang, X. Liao, B. Shi, Hg(II) removal from aqueous solution by bayberry tannin-immobilized collagen fiber, J. Hazard. Mater. 170 (2009) 1141–1148.
[12] B.K. Wong, V.S. Lai, J. Lam, A bibliography of neural network business application research: 1994–1998, Comput. Oper. Res. 27 (2000) 1045–1076.
[13] I. Anagu, J. Ingwersen, J. Utermann, T. Streck, Estimation of heavy metal sorption in German soils using artificial neural networks, Geoderma 152 (2009) 104–112.
[14] K. Yetilmezsoy, S. Demirel, Artificial neural network (ANN) approach for modeling of Pb(II) adsorption from aqueous solution by Antep pistachio (*Pistacia vera* L.) shells, J. Hazard. Mater. 153 (2008) 1288–1300.
[15] M.N. Kashani, J. Aminian, S. Shahhosseini, M. Farrokhi, Dynamic crude oil fouling prediction in industrial preheaters using optimized ANN based moving window technique, Chem. Eng. Res. Des. 90 (2012) 938–949.

[16] A. Akkoyunlu, K. Yetilmezsoy, D. Erturk, E. Oztemel, A neural network-based approach for the prediction of urban SO_2 concentrations in the Istanbul metropolitan area, Int. J. Environ. Pollut. 40 (2010) 301–321.
[17] D.M. Himmelblau, Applications of artificial neural networks in chemical engineering, Korean J. Chem. Eng. 17 (2000) 373–392.
[18] K.V. Kumar, M. de Castro, M. Martinez-Escandell, M. Molina-Sabio, F. Rodriguez-Reinoso, Neural network and principal component analysis for modeling of hydrogen adsorption isotherms on KOH activated pitch-based carbons containing different heteroatoms, Chem. Eng. J. 159 (2010) 272–279.
[19] A.R. Khataee, M. Zarei, M. Pourhassan, Bioremediation of Malachite Green from contaminated water by three microalgae: Neural network modeling, Clean 38 (2010) 96–103.
[20] W.J. Lau, A.F. Ismail, Polymeric nanofiltration membranes for textile dye wastewater treatment: Preparation, performance evaluation, transport modelling, and fouling control-a review, Desalination 245 (2009) 321–348.
[21] D. Aguado, A. Ferrer, A. Seco, J. Ferrer, Comparison of different predictive models for nutrient estimation in a sequencing batch reactor for wastewater treatment, Chemom. Intell. Lab. Syst. 84 (2006) 75–81.
[22] N. Basant, S. Gupta, A. Malik, K.P. Singh, Linear and nonlinear modeling for simultaneous prediction of dissolved oxygen and biochemical oxygen demand of the surface water—A case study, Chemom. Intell. Lab. Syst. 104 (2010) 172–180.
[23] K.P. Singh, A. Basant, A. Malik, G. Jain, Artificial neural network modeling of the river water quality—A case study, Ecol. Modell. 220 (2009) 888–895.
[24] H. Moral, A. Aksoy, C.F. Gokcay, Modeling of the activated sludge process by using artificial neural networks with automated architecture screening, Comput. Chem. Eng. 32 (2008) 2471–2478.
[25] W.B. Chen, W.C. Liu, M.H. Hsu, Comparison of ANN approach with 2D and 3D hydrodynamic models for simulating estuary water stage, Adv. Eng. Softw. 45 (2012) 69–79.
[26] E. Tomczak, Application of ANN and EA for description of metal ions sorption on chitosan foamed structure-equilibrium and dynamics of packed column, Comput. Chem. Eng. 35 (2011) 226–235.
[27] K.V. Kumar, K. Porkodi, Modelling the solid–liquid adsorption processes using artificial neural networks trained by pseudo second order kinetics, Chem. Eng. J. 148 (2009) 20–25.
[28] M.R. Fagundes-Klen, P. Ferri, T.D. Martins, C.R.G. Tavares, E.A. Silva, Equilibrium study of the binary mixture of cadmium–zinc ions biosorption by the *Sargassum filipendula* species using adsorption isotherms models and neural network, Biochem. Eng. J. 34 (2007) 136–146.
[29] K.V. Shetty, S. Nandennavar, G. Srinikethan, Artificial neural networks model for the prediction of steady state phenol biodegradation in a pulsed plate bioreactor, J. Chem. Technol. Biotechnol. 83 (2008) 1181–1189.
[30] D.K. Chaturvedi, Soft Computing: Techniques and its Applications in Electrical Engineering, Studies in Computational Intelligence, Springer, Berlin, 2008.
[31] M. Riedmiller, H. Braun, A direct adaptive method for faster backpropagation learning: The RPROP algorithm neural networks, *IEEE Int. Conf.* (1993) 586–591.
[32] S. Nissen, Implementation of a fast artificial neural network library (FANN), Department of Computer Science University of Copenhagen (DIKU), Technical Report, 2003.
[33] C. Igel, M. Hüsken, Improving the Rprop learning algorithm, in: H. Bothe, R. Rojas (Eds.), Proceedings of the Second International Symposium on Neural Computation, NC'2000, ICSC Academic Press, Canada/Switzerland, 2000, pp. 115–121.
[34] S. Nissen, Fast artificial neural network library. Available from: http://leenissen.dk/fann/wp/ (accessed 1 July 2012).
[35] Tool for the Fast Artificial Neural Network Library (FANN). Available from: http://code.google.com/p/fanntool/ (accessed 1 July 2012).
[36] K.P. Moustris, I.K. Larissi, P.T. Nastos, A.G. Paliatsos, Precipitation forecast using artificial neural networks in specific regions of Greece, Water Res. Manage. 25 (2011) 1979–1993.
[37] P. Chaves, F.J. Chang, Intelligent reservoir operation system based on evolving artificial neural networks, Adv. Water Res. 31 (2008) 926–936.
[38] Y.H. Chen, F.J. Chang, Evolutionary artificial neural networks for hydrological systems forecasting, J. Hydrol. 367 (2009) 125–137.
[39] S. Mohanty, M.K. Jha, A. Kumar, K.P. Sudheer, Artificial neural network modeling for groundwater level forecasting in a River Island of Eastern India, Water Res. Manage. 24 (2010) 1845–1865.
[40] V. Nourani, M. Komasi, A. Mano, A multivariate ANN-wavelet approach for rainfall–runoff modeling, Water Res. Manage. 23 (2009) 2877–2894.
[41] M.M. Hamed, M.G. Khalafallah, E.A. Hassanien, Prediction of wastewater treatment plant performance using artificial neural networks, Environ. Modell. Softw. 19 (2004) 919–928.
[42] S.K. Behera, E.R. Rene, H.S. Park, Neural network modeling of sorption of pharmaceuticals in engineered floodplain filtration system, Expert Syst. Appl. 39 (2012) 6052–6060.
[43] X. Su, G. Zeng, G. Huang, J. Li, J. Liang, L. Wang, C. Du, Modeling research on the sorption kinetics of pentachlorophenol (PCP) to sediments based on neural networks and neuro-fuzzy systems, Eng. Appl. Artif. Intell. 20 (2007) 239–247.
[44] F. Nakhaei, M.R. Mosavi, A. Sam, Y. Vaghei, Recovery and grade accurate prediction of pilot plant flotation column concentrate: Neural network and statistical techniques, Int. J. Miner. Process. 110–111 (2012) 140–154.
[45] T.N. Singh, V.K. Singh, S. Sinha, Prediction of cadmium removal using an artificial neural network and a neuro-fuzzy technique, Mine Water Environ. 25 (2006) 214–219.
[46] T. Shojaeimehr, F. Rahimpour, M.A. Khadivi, M. Sadeghi, A modeling study by response surface methodology (RSM) and artificial neural network (ANN) on Cu^{2+} adsorption optimization using light expended clay aggregate (LECA), J. Ind. Eng. Chem. 20 (2014) 870–880.

[47] M.F. Ahmad, S. Haydar, A.A. Bhatti, A.J. Bari, Application of artificial neural network for the prediction of biosorption capacity of immobilized Bacillus subtilis for the removal of cadmium ions from aqueous solution, Biochem. Eng. J. 84 (2014) 83–90.
[48] U. Ozdemir, B. Ozbay, S. Veli, S. Zor, Modeling adsorption of sodium dodecyl benzene sulfonate (SDBA) onto polyaniline (PANI) by using multi linear regression and artificial neural networks, Chem. Eng. J. 178 (2011) 183–190.
[49] A.K. Giri, R.K. Patel, S.S. Mahapatra, Artificial neural network (ANN) approach for modelling of arsenic (III) biosorption from aqueous solution by living cells of *Bacillus cereus* biomass, Chem. Eng. J. 178 (2011) 15–25.
[50] S.H. Asl, M. Ahmadi, M. Ghiasvand, A. Tardast, R. Katal, Artificial neural network (ANN) approach for modeling of Cr(VI) adsorption from aqueous solution by zeolite prepared from raw fly ash (ZFA), J. Ind. Eng. Chem. 19 (2013) 1044–1055.